

Primordial black hole dark matter from catastrogenesis with unstable pseudo-Goldstone bosons

Graciela B. Gelmini,^a Jonah Hyman,^a Anna Simpson^a
and Edoardo Vitagliano^b

^aDepartment of Physics and Astronomy, University of California, Los Angeles,
475 Portola Plaza, Los Angeles, CA 90095-1547, U.S.A.

^bRacah Institute of Physics, Hebrew University of Jerusalem,
Edmond J. Safra Campus, Jerusalem 9190401, Israel

E-mail: gelmini@physics.ucla.edu, jthyman@physics.ucla.edu, ansimps@g.ucla.edu,
edoardo.vitagliano@mail.huji.ac.il

Received April 4, 2023

Revised May 28, 2023

Accepted June 8, 2023

Published June 26, 2023

Abstract. We propose a new scenario for the formation of asteroid-mass primordial black holes (PBHs). Our mechanism is based on the annihilation of the string-wall network associated with the breaking of a $U(1)$ global symmetry into a discrete Z_N symmetry. If the potential has multiple local minima ($N > 1$) the network is stable, and the annihilation is guaranteed by a bias among the different vacua. The collapse of the string-wall network is accompanied by *catastrogenesis*, a large production of pseudo-Goldstone bosons (pGBs) — e.g. axions, ALPs, or majorons — gravitational waves, and PBHs. If pGBs rapidly decay into products that thermalize, as predicted e.g. in the high-quality QCD axion and heavy majoron models, they do not contribute to the dark matter population, but we show that PBHs can constitute 100% of the dark matter. The gravitational wave background produced by catastrogenesis with heavy unstable axions, ALPs, or majorons could be visible in future interferometers.

Keywords: axions, Cosmic strings, domain walls, monopoles, particle physics - cosmology connection, primordial black holes

ArXiv ePrint: [2303.14107](https://arxiv.org/abs/2303.14107)



Contents

1	Introduction	1
2	ALP models and their cosmology	2
3	Primordial black holes	5
4	Potentially observable GWs	11
5	Self consistency conditions	13
6	Concluding remarks	15
A	Brief derivation of the present GW energy density	16

1 Introduction

The only known interaction that dark matter (DM) has with ordinary matter is gravitational [1, 2]. This is why black holes can be good DM candidates if they are formed in the early Universe, i.e. are primordial black holes (PBHs) [3–8]. Moreover, they need to be stable, so that they do not evaporate through Hawking’s radiation before the present time [9–14], and they need to avoid current constraints from microlensing [15–17], as well as many other bounds collected in e.g. ref. [18]. There is a window of PBH masses, between 10^{-16} and $10^{-10} M_{\odot}$ (roughly equivalent to asteroid masses), for which PBHs can constitute 100% of DM. A necessarily incomplete list of proposed formation scenarios for PBHs in the asteroid-mass range includes density perturbations in the early Universe (see e.g. [6, 19–21]), bubble collisions [22, 23], the collapse of cosmic strings [24], scalar field dynamics [25–28], long-range interactions [29], and collapse of domain walls [30, 31] or vacuum bubbles [32, 33] in multi-field inflationary scenarios. We propose here a novel production scenario for asteroid-mass PBHs based on the mechanism we have dubbed catastrogenesis in our previous work [34]. Our mechanism does not depend on inflationary physics, nor on primordial density perturbations, and crucially it can be linked to other unsolved problems in particle physics, e.g. the strong CP problem.

We assume the existence of a global U(1) symmetry whose spontaneous breaking is associated with the existence of Goldstone bosons. A generic feature of these models is that the global symmetry is also broken explicitly, so that the bosons are massive, i.e. pseudo-Goldstone bosons (pGBs). This happens in a plethora of extensions of the Standard Model of particle physics, including the original axion model [35–37], invisible axion (also called QCD axion) models [38–40], generic axion-like particle (ALP) models [41], and (singlet) majoron models [42–48]. Intriguingly, some models predict a larger-than-expected mass for the QCD axion [49–52], including the so-called “high-quality QCD axion” [53] and previous models. (For a review on earlier attempts of model building predicting heavy QCD axions, see section 6.7 of ref. [54].) Heavy majorons, even of mass in the TeV range, have been considered as well (see e.g. [44, 47]). If the pGBs are unstable and decay in the early Universe, they could not constitute the DM, and thus such models might lack a DM candidate. This can be the case for axions and ALPs, as well as for majorons which could get a mass from soft breaking terms or from gravitational effects (see e.g. [43–47]).

The stability of these pGBs depends on their mass and couplings. Axion-like particles with a coupling to photons are probed by beam-dump experiments [55–59], supernovae [60–66] and

neutron star mergers [67] up to several hundreds MeV, while cosmological observations [68, 69] reach even larger masses, above a TeV, for very small couplings [68, 69]. Colliders can exclude masses up to the TeV scale [70, 71], though only for large couplings (this implies e.g. an open window for the high-quality QCD axion [53]). Assuming couplings to leptons, there are bounds from beam dumps [71] and astrophysical observations [63, 72], but the parameter space is largely unconstrained above the GeV scale.¹ Heavy majorons are similarly probed by cosmology [74], supernovae [75], and laboratory searches [76–78], which again leave masses above 1 GeV largely unconstrained.

We deal with bosons that are heavier than a GeV and decay very early into Standard Model products which rapidly thermalize. Axions would decay into photons and charged fermions. Majorons could decay mostly into two relatively heavy right-handed neutrinos, which in turn decay very fast into pions, charged fermion pairs, and active neutrinos. Therefore, such pGBs cannot be the DM in the models we consider, but catastrogenesis [34] may lead to a different DM candidate, namely PBHs. We consider explicit breaking potentials which admit a number $N > 1$ of minima along the orbit of vacua. In this case, if inflation happens before the spontaneous symmetry breaking, as we assume, a cosmological problem may arise: a stable string-wall network forms and could eventually come to dominate the Universe leading to an unacceptable cosmology [79, 80]. Both axion [81] and majoron [45] models can result in $N > 1$.

The cosmological problem is solved by adding an additional explicit breaking in the Lagrangian [81–83], possibly due to the effect of Planck suppressed operators [34, 84, 85], which produces an energy difference (a bias) between the minima that leads to a unique vacuum. As first proposed in 1974 in ref. [79], this small bias results in the annihilation of the string-wall network, and only one vacuum is eventually left. The annihilation is accompanied by catastrogenesis [34], i.e. the production of gravitational waves (GWs), pGBs, and PBHs. Our main result is that for a range of the string-wall network annihilation temperatures, one can form asteroid-mass PBHs and potentially a GW signal in future observatories. As we will see, both the abundance of PBHs and the amplitude of the stochastic GW background produced depend crucially on the details of the annihilation.

Although we focus on models featuring pGBs (that we will call, as customary in the recent literature, ALPs), our mechanism also applies in principle to the breaking of any discrete symmetry with multiple vacua, when the wall system annihilation produces unstable particles, such as flavons [86], whose decay products thermalize.

The paper is structured as follows. In section 2 we introduce the generic particle model we assume and describe its cosmology. In section 3 we present our estimates for the PBH relic abundance and find the range of parameters in which they could account for the whole of the DM. In section 4 we show that for the same range of parameters a signal in GWs could be observable in future detectors. Section 5 explains in detail restrictions imposed by consistency conditions of our model. Finally the last section contains some concluding remarks.

2 ALP models and their cosmology

Here we briefly review well-known aspects of the models we study. A more detailed account can be found e.g. in ref. [34] (see also [87]). We consider a complex scalar field $\phi = |\phi|e^{i\theta}$ whose phase after spontaneous symmetry breaking at an energy scale V is related to the ALP field a as $a = \theta V$. The generic potential $V(\phi)$ for the scalar field includes three terms, one

¹A collection of bounds on axions and axion-like particles can be found in ref. [73].

with a spontaneously broken global U(1) symmetry and two others which break the symmetry explicitly,

$$V(\phi) \supset \frac{\lambda}{4}(|\phi|^2 - V^2)^2 + \frac{v^4}{2} \left(1 - \frac{|\phi|}{V} \cos(N\theta) \right) - \epsilon_b v^4 \frac{|\phi|}{V} \cos(\theta - \delta), \quad (2.1)$$

with $V \gg v$. The first term is U(1) invariant and leads to the spontaneous breaking of this symmetry during a phase transition in the early Universe, at which the magnitude of the field becomes $|\phi| \simeq V$ and cosmic strings are produced due to the random distribution of the phase θ in different correlation volumes. Assuming that the bosons have the same average energy of the visible sector (which is possible in many inflation models), this phase transition happens at a temperature $T \simeq V$. Upper bounds on the energy scale of inflation impose $V \lesssim 10^{16}$ GeV [88, 89]. A short time after its formation, the string system enters into a “scaling” regime, in which the population of strings in a Hubble volume tends to remain of $\mathcal{O}(1)$ (see e.g. ref. [80] and references therein).

The second term in eq. (2.1) explicitly breaks the U(1) symmetry of the first term into a Z_N discrete subgroup, producing N degenerate vacua along the previous U(1) orbit of minima $|\phi| \simeq V$. Close to each minimum the ALP field a has a mass

$$m_a \simeq \frac{v^2 N}{\sqrt{2}V}. \quad (2.2)$$

We assume for simplicity that temperature corrections to m_a are negligible. We do not expect that these corrections will be important in our scenario since, as we explain below, catastrogenesis is independent of the temperature dependence as it happens when the ALP mass has reached its asymptotic present value.

The equation of motion of the field a in the expanding Universe is that of a harmonic oscillator with damping term $3H\dot{a}$, where $H = (2t)^{-1}$ is the Hubble expansion rate during the radiation dominated epoch. While $3H \gg m_a$ the field does not change with time. As H decreases with time, at a temperature T_w when $H(T_w) \simeq m_a/3$, regions of the Universe with different values of θ evolve to different minima separated by domain walls of mass per unit surface (or surface tension)

$$\sigma \simeq f_\sigma v^2 \frac{V}{N}. \quad (2.3)$$

Here f_σ is a model dependent dimensionless parameter. For $N = 2$ the model is solvable analytically and $f_\sigma \simeq 6$. Whenever choosing specific values of N and f_σ will be required, we will assume $N = 6$ and $f_\sigma/N \simeq 1$.

The temperature T_w at which walls appear, i.e. $H(T_w) \simeq m_a/3$, is

$$T_w \simeq \frac{1.6 \times 10^9 \text{ GeV}}{[g_\star(T_w)]^{1/4}} \left(\frac{m_a}{\text{GeV}} \right)^{1/2}, \quad (2.4)$$

where we have used that for a radiation dominated Universe the Hubble expansion rate is

$$H(T) = \sqrt{\frac{8\pi^3 g_\star(T)}{90}} \frac{T^2}{M_{\text{P}}}. \quad (2.5)$$

Here, $M_{\text{P}} = 1.22 \times 10^{19}$ GeV is the Planck mass and g_\star is the energy density number of degrees of freedom [90].

A short time after walls form, when friction of the walls with the surrounding medium is negligible, the string-wall system enters into another scaling regime in which the linear size of the walls is the cosmic horizon size $\simeq t$. Therefore, its energy density at time t is

$$\rho_{\text{wall}} \simeq \frac{\sigma}{t}. \quad (2.6)$$

Friction on walls, due to scattering with particles in the surrounding medium, is negligible when the energy of these particles is much larger than the ALP mass m_a [91, 92], which is the case for most if not all the models we consider. This has been confirmed e.g. in ref. [93]. There the impact of friction on the parameter space of the high-quality QCD axion was studied (see their appendix D), and it was concluded that even when friction was important their results were only mildly different from those obtained neglecting friction.

The third term in eq. (2.1), proposed in ref. [81], is assumed to be much smaller than the second one, i.e. $\epsilon_b \ll 1$. It breaks explicitly the Z_N symmetry, raising all vacua with respect to the lowest energy one by a bias of order

$$V_{\text{bias}} \simeq \epsilon_b v^4. \quad (2.7)$$

The motion of the walls after they are formed is determined by two quantities. The surface tension σ tends to straighten out curved walls to the horizon scale as it produces a pressure $p_T \simeq \rho_{\text{wall}}$, while the bias produces a volume pressure $p_V \simeq V_{\text{bias}}$ [83]. This latter pressure tends to accelerate the walls towards their higher energy adjacent vacuum, converting the higher energy vacuum into the lower energy one, which releases energy that fuels the wall motion.

Assuming that $p_V \ll p_T$ when walls form (i.e. $\epsilon_b \ll 1$), as p_T decreases with time it becomes similar to and then smaller than p_V . At this point the bias drives the walls (and strings bounding them) to annihilation. Taking $p_T \simeq p_V$, i.e. $\rho_{\text{wall}} \simeq \sigma/t_{\text{ann}} \simeq V_{\text{bias}} \simeq \epsilon_b v^4$, as the condition for wall annihilation,

$$H(T_{\text{ann}}) = \frac{1}{2t_{\text{ann}}} \simeq \frac{V_{\text{bias}}}{2\sigma} \simeq \frac{\epsilon_b m_a}{\sqrt{2} f_\sigma}, \quad (2.8)$$

which defines the temperature T_{ann} at which the string-wall system annihilates,

$$T_{\text{ann}} \simeq \frac{1.9 \times 10^9 \text{ GeV}}{[g_\star(T_{\text{ann}})]^{1/4}} \sqrt{\frac{V_{\text{bias}}}{\sigma \text{ GeV}}} \simeq \frac{2.2 \times 10^9 \text{ GeV}}{[g_\star(T_{\text{ann}})]^{1/4}} \sqrt{\frac{\epsilon_b m_a}{f_\sigma \text{ GeV}}}. \quad (2.9)$$

At this point the energy stored in the string-wall system goes almost entirely into non-relativistic or mildly relativistic ALPs (since the wall thickness is $\simeq m_a^{-1}$) [94], into GWs, and into PBHs.

The GWs produced at annihilation (see appendix A and e.g. ref. [34] for more details) have a characteristic spectrum peaked at

$$f_{\text{peak}} \simeq 0.76 \text{ Hz} \frac{T_{\text{ann}}}{10^7 \text{ GeV}} \frac{[g_\star(T_{\text{ann}})]^{1/2}}{[g_{s\star}(T_{\text{ann}})]^{1/3}}, \quad (2.10)$$

and peak energy density (see e.g. [95–98])

$$\Omega_{\text{GW}} h^2|_{\text{peak}} \simeq \epsilon_{\text{GW}} \frac{1.2 \times 10^{-79} g_\star(T_{\text{ann}}) \sigma^4}{[g_{s\star}(T_{\text{ann}})]^{4/3} V_{\text{bias}}^2 \text{ GeV}^4} \simeq \epsilon_{\text{GW}} \frac{1.2 \times 10^{-79} g_\star(T_{\text{ann}})}{\epsilon_b^2 [g_{s\star}(T_{\text{ann}})]^{4/3}} \left(\frac{f_\sigma V}{N \text{ GeV}} \right)^4. \quad (2.11)$$

Following ref. [98], we include in eq. (2.11) a dimensionless factor $\epsilon_{\text{GW}} \simeq 10 - 20$ for $N = 6$ (see figure 8 of ref. [98]) found in numerical simulations that parameterizes the efficiency of GW production. In the following we conservatively assume $\epsilon_{\text{GW}} = 10$.

Eq. (2.11) is also (see appendix A) the usually quoted maximum of the GW energy density spectrum at present as a function of the wave-number at present k , which for the present scale factor $R_0 = 1$ coincides with the comoving wave-number, or of the frequency $f = k/(2\pi)$. This is defined as $\Omega_{\text{GW}} h^2(k, t_0) = [h^2/\rho_c(t_0)] (d\rho_{\text{GW}}(t)/d\ln k)_0 = [h^2/\rho_c(t_0)] \sigma^2/M_{\text{P}}^2$ [86, 99].

GWs are also emitted by the string network before walls appear. The dominant source of these waves are loops continuously formed by string fragmentation. From the spectra computed in refs. [100–102], also based on the quadrupole formula, a simple good fit can be derived for the energy spectrum of GWs emitted by strings during the radiation dominated era, namely

$$\Omega_{\text{GW}}^{\text{st}} h^2 \simeq 3.6 \times 10^{-9} \left(\frac{10^2 \text{ Hz}}{f} \right)^{1/8} \left(\frac{V}{10^{16} \text{ GeV}} \right)^4. \quad (2.12)$$

This spectrum has a low frequency cutoff $f_{\text{cut}}^{\text{st}}$ at the frequency of GWs emitted the latest possible by strings, when the horizon size is largest, namely when walls are formed, which is given by eq. (2.10) using T_{w} instead of T_{ann} , i.e.

$$f_{\text{cut}}^{\text{st}} \simeq \frac{T_{\text{w}}}{T_{\text{ann}}} f_{\text{peak}} \frac{[g_{\star}(T_{\text{w}})]^{1/2} [g_{s\star}(T_{\text{ann}})]^{1/3}}{[g_{s\star}(T_{\text{w}})]^{1/3} [g_{\star}(T_{\text{ann}})]^{1/2}}, \quad (2.13)$$

which can be written in terms of the ALP mass as

$$f_{\text{cut}}^{\text{st}} \simeq 82 \text{ Hz} \left(\frac{m_a}{\text{GeV}} \right)^{1/2} \left[\frac{g_{\star}(T_{\text{w}})}{105} \right]^{1/4} \left[\frac{105}{g_{s\star}(T_{\text{w}})} \right]^{1/3}. \quad (2.14)$$

Given that we consider only ALPs with mass $m_a \gtrsim 1 \text{ GeV}$, the emission of GWs by strings before walls appear only contributes at high frequencies, $f \gtrsim 82 \text{ Hz}$. Comparing eqs. (2.12) and (2.11) we are going to show that only in a restricted parameter space GWs from strings could be observable by the future GW Einstein Telescope [103].

In the next section we will argue that when ALPs are unstable and decay fast in the early Universe, the string-wall system annihilation could produce PBHs that account for the whole (or part) of the dark matter, while also producing GWs with peak frequency from 10^{-5} to 10^2 Hz and density $\Omega_{\text{GW}} h^2 > 10^{-15}$, which corresponds to an observable signal in future GW detectors.

3 Primordial black holes

In $N = 1$ models the walls appear in the form of ribbons flanked by two strings which become narrower due to surface tension and disappear very fast. By contrast, in the latest stages of wall annihilation in $N > 1$ models, closed walls are expected to arise and collapse in an approximately spherically symmetric way. In this case, some fraction of the closed walls could shrink to their Schwarzschild radius $R_{\text{Sch}}(t) = 2GM(t) = 2M(t)/M_{\text{P}}^2$ and collapse into PBHs [104]. Here $M(t)$ is the mass within the collapsing closed wall at time t . Considering that during the scaling regime the typical linear size of the walls is the horizon size, which we take to be $\simeq t$, PBH formation could happen if the ratio

$$p(t) = \frac{R_{\text{Sch}}(t)}{t} = \frac{2M(t)}{t M_{\text{P}}^2} \quad (3.1)$$

is close to one, i.e. $p(t) \simeq 1$. Simulations of the annihilation process [105] can then be used to estimate at which temperature $T_\star \lesssim T_{\text{ann}}$ this could happen.

As we mentioned above, the annihilation process starts at T_{ann} when the contribution of the volume energy density to the mass within a closed wall of radius t becomes as important as the contribution of the wall energy density. Shortly after, the volume density term dominates over the surface term, and the volume pressure accelerates the walls towards each other. Close to the start of the annihilation process, the mass within a closed wall as a function of the lifetime t of the Universe is

$$M(t) \simeq \frac{4}{3}\pi t^3 V_{\text{bias}} + 4\pi t^2 \sigma. \quad (3.2)$$

Therefore, the ratio $p(t)$ increases with time (as t^2 once the volume term becomes dominant). At $T > T_{\text{ann}}$ the surface term dominates and at $T < T_{\text{ann}}$ the volume term dominates. If at the moment t_{ann} when annihilation starts $p(t_{\text{ann}})$ is close to 1, PBHs would form immediately. If $p(t_{\text{ann}}) \ll 1$ instead, PBHs could only form later, at a time $t_\star > t_{\text{ann}}$ corresponding to a temperature $T_\star < T_{\text{ann}}$, for which $p(t_\star) = 1$. Temperature and time are related by $H = 1/2t$ (see eq. (2.5)), assuming radiation domination. If $p(t_{\text{ann}}) \ll 1$, at T_\star only a small fraction of the original string-wall system still remains.

The wall surface energy density σ/t decreases with time with respect to the volume energy density due to the bias V_{bias} which is constant in time. Although the volume energy density is negligible initially, both contributions become similar at T_{ann} , i.e. $V_{\text{bias}} \simeq \sigma/t_{\text{ann}}$, thus eq. (3.2) implies

$$M(t_{\text{ann}}) \simeq \frac{16}{3}\pi t_{\text{ann}}^3 V_{\text{bias}}, \quad (3.3)$$

so that the ratio $p(t)$ in eq. (3.1) becomes

$$p(T_{\text{ann}}) \simeq \frac{30}{\pi^2} \frac{V_{\text{bias}}}{g_\star(T_{\text{ann}}) T_{\text{ann}}^4}. \quad (3.4)$$

As expected of all quantities depending only on the annihilation process, $M(t_{\text{ann}})$ and $p(T_{\text{ann}})$ only depend on the parameters V_{bias} and σ . After t_{ann} , the volume contribution to the density rapidly becomes dominant over the surface contribution, and

$$M(t) \simeq \frac{4}{3}\pi t^3 V_{\text{bias}} \left(1 + 3 \frac{t_{\text{ann}}}{t}\right), \quad (3.5)$$

thus

$$p(T) \simeq \frac{p(T_{\text{ann}})}{4} \left(\frac{t}{t_{\text{ann}}}\right)^2 \left(1 + 3 \frac{t_{\text{ann}}}{t}\right). \quad (3.6)$$

When $t \gg 3 t_{\text{ann}}$ we can neglect the second term in eqs. (3.5) and (3.6), consequently

$$p(T) \simeq \frac{p(T_{\text{ann}})}{4} \frac{g_\star(T_{\text{ann}})}{g_\star(T)} \left(\frac{T_{\text{ann}}}{T}\right)^4. \quad (3.7)$$

We are here assuming that the characteristic linear dimension of the walls continues to be close to t even after annihilation is underway. At some point along this process one expects larger deviations from this scaling behavior, but detailed simulations that are not available at the moment would be needed to assess when and how this departure happens. Using eq. (3.7) we find the PBH formation temperature T_\star as the temperature at which $p(T_\star) = 1$, which in terms of T_{ann} is

$$p(T_\star) \simeq \frac{p(T_{\text{ann}})}{4} \frac{g_\star(T_{\text{ann}})}{g_\star(T_\star)} \left(\frac{T_{\text{ann}}}{T_\star}\right)^4 = 1. \quad (3.8)$$

This relation defines T_\star and its corresponding time $t_\star = 1/2H(T_\star)$. The PBH mass is then $M(t_\star)$,

$$M_{\text{PBH}} = M(t_\star) \simeq \frac{4\pi}{3} V_{\text{bias}} t_\star^3 \simeq \frac{2}{[p(T_{\text{ann}})]^{3/2}} M(t_{\text{ann}}) \simeq \left(\frac{3}{32\pi}\right)^{1/2} \frac{M_{\text{P}}^3}{V_{\text{bias}}^{1/2}}. \quad (3.9)$$

Eqs. (3.8) and (3.9) show that the temperature of PBH formation T_\star depends only on V_{bias} (or, equivalently, M_{PBH})

$$T_\star \simeq 0.9 \text{ GeV} \left[\frac{V_{\text{bias}}}{\text{GeV}^4 g_\star(T_\star)} \right]^{1/4} \simeq \frac{0.5 \text{ GeV}}{[g_\star(T_\star)]^{1/4}} \left(\frac{M_\odot}{M_{\text{PBH}}} \right)^{1/2}. \quad (3.10)$$

From eq. (3.9) and eq. (3.1) one finds

$$p(T_{\text{ann}}) \simeq \frac{t_{\text{ann}}^2 M_{\text{P}}^4}{M_{\text{PBH}}^2} = \frac{90}{32\pi^3} \frac{1}{g_\star(T_{\text{ann}})} \frac{M_{\text{P}}^6}{T_{\text{ann}}^4 M_{\text{PBH}}^2} = \frac{2.4 \times 10^{-33}}{g_\star(T_{\text{ann}})} \left(\frac{\text{GeV}}{T_{\text{ann}}} \right)^4 \left(\frac{10^{16} M_\odot}{M_{\text{PBH}}} \right)^2. \quad (3.11)$$

Small deviations from a spherically symmetric collapse, as well as effects of some angular momentum, could make the probability of forming a PBH at temperature T somewhat smaller than $p(T)$, which we could attempt to parameterize as $p(T)^\beta$ with a real positive exponent β . A modification of the probability of this type does not have any effect on our estimates of PBH formation, since when $p = 1$ also $p^\beta = 1$. A large enough deviation from the spherical shape could prevent the formation of a PBH, since the degree of asymmetry may decrease initially during the contraction but increase in the late stages of the collapse [106]. The details of the collapse process become more important if $p(T_{\text{ann}}) \ll 1$, since a longer evolution is needed to potentially reach $p = 1$ (ref. [104] suggests that in this case asphericities, energy losses or angular momentum might make more difficult the formation of a black hole). However, a large deviation from sphericity is unlikely, as shown in the context of the collapse of vacuum bubbles produced during inflation [32]. Thus, at least for some portion of the walls, the departure from spherical symmetry during collapse is likely to be small. In this case, the PBH density at formation is given by the energy density in the wall system when PBHs form times the probability of PBH formation, namely

$$\rho_{\text{PBH}}(T_\star) \simeq p^\beta(T_\star) \rho_{\text{wall}}(T_\star), \quad (3.12)$$

and the fraction f_{PBH} of the total DM density ρ_{DM} in PBHs is

$$f_{\text{PBH}} = \frac{\rho_{\text{PBH}}(T_\star)}{\rho_{\text{DM}}(T_\star)} \simeq p^\beta(T_\star) \frac{\rho_{\text{wall}}(T_\star)}{\rho_{\text{DM}}(T_\star)} = \frac{\rho_{\text{wall}}(T_\star)}{\rho_{\text{wall}}(T_{\text{ann}})} \frac{\rho_{\text{wall}}(T_{\text{ann}})}{\rho_{\text{DM}}(T_\star)}, \quad (3.13)$$

where we used that at the moment of PBH formation temperature $p(T_\star) = 1$. Notice that f_{PBH} is the same at present as it was at T_\star (since the PBH and DM densities redshift in the same manner).

Simulations of the process of the string-wall system annihilation for $N > 1$ models have been performed [105], which provided measurements of the times at which the area density of walls (area per unit volume A/V) is 10% and 1% of what it would have been without a bias. Notice that this ratio is the same in comoving (as given in ref. [105]) or physical coordinates. We call these times $t(10\%)$ and $t(1\%)$, and the corresponding temperatures $T(10\%)$ and $T(1\%)$. In ref. [105], the pressure due to the walls is parameterized as $\mathcal{A}(t)\sigma/t$,

where $\mathcal{A}(t)$ is a function which accounts for deviations from scaling, and find that $\mathcal{A}(t)$ is close to 1. Assuming that the wall contribution to the energy density is dominant, a simple approximation as a power law for the evolution of the wall energy density with temperature after annihilation starts,

$$\frac{\rho_{\text{wall}}(T)}{\rho_{\text{wall}}(T_{\text{ann}})} = \left(\frac{T}{T_{\text{ann}}}\right)^\alpha, \quad (3.14)$$

seems to work well to extract the real positive exponent α from the mentioned simulations [105].

Table VI and figure 4 of ref. [105] show that the $t(1\%)/t(10\%) = [T(10\%)/T(1\%)]^2$ ratio takes up central values close to 2, actually from 1.7 to 1.5, under different assumptions. If the energy of the string-wall system is still dominated by the contribution of the walls until $t(1\%)$, i.e. the energy density is proportional to A/V , $\rho_{\text{wall}} = A\sigma/V$, then

$$\left(\frac{T(10\%)}{T(1\%)}\right)^\alpha \simeq \frac{\rho_{\text{wall}}(T(10\%))}{\rho_{\text{wall}}(T(1\%))} = \frac{\frac{A}{V}\Big|_{t(10\%)}}{\frac{A}{V}\Big|_{t(1\%)}} = 10 \left(\frac{t(1\%)}{t(10\%)}\right), \quad (3.15)$$

and the central values measured of the $t(1\%)/t(10\%)$ ratio translate into values of the exponent α roughly between 9 and 14. In our figures we include also the value 7 used in ref. [104]. Taking into account the systematic errors quoted in table VI of ref. [105], α could be as large as 21. However, the volume contribution to the energy density of the string-wall system may not be negligible, which introduces a further uncertainty in the determination of α . To get an estimate of this uncertainty, we can proceed assuming that the volume energy is dominant in the string-wall system, i.e. that its density is proportional to $A^{3/2}$. In fact, since the simulation volume in ref. [105] is the same in both the cases with and without a bias (in the latter case the evolution follows the scaling solution), the ratio of the area densities can be identified with the ratio of the area A in the evolution with bias and the characteristic area $\simeq t^2$ in the scaling case within a Hubble volume. Thus $[A(t(10\%))]^{1/2} \simeq \sqrt{0.10} t(10\%)$, and similarly $[A(t(1\%))]^{1/2} \simeq \sqrt{0.01} t(1\%)$. Moreover, in a Hubble volume, if the V_{bias} contribution dominates over the surface energy, the wall-system density is $\rho_{\text{wall}} \simeq V_{\text{bias}}[A(t)]^{3/2}/t^3$, and

$$\left(\frac{T(10\%)}{T(1\%)}\right)^\alpha \simeq \frac{\rho_{\text{wall}}(T(10\%))}{\rho_{\text{wall}}(T(1\%))} \simeq 10^{3/2}. \quad (3.16)$$

This leads to values of α larger by a factor $3/2$ with respect to our previous estimates minus two (i.e. from $(3/2)7$ to $(3/2)19$). Thus, α could be as large as 28.

Using eq. (3.14), eq. (3.13) becomes

$$f_{\text{PBH}} \simeq \left(\frac{T_\star}{T_{\text{ann}}}\right)^\alpha \frac{\rho_{\text{wall}}(T_{\text{ann}})}{\rho_{\text{DM}}(T_\star)}. \quad (3.17)$$

In this equation $\rho_{\text{DM}}(T_\star)$ is easily related by redshift to the present dark matter density, and $\rho_{\text{wall}}(T_{\text{ann}})$ can be related to the present radiation density, in the following manner.

Had the string-wall system not annihilated, its energy density would have continued evolving in the scaling regime, with $\rho_{\text{wall}} \simeq \sigma/t$, until the time t_{wd} at which $\rho_{\text{wall}}(t_{\text{wd}}) = \rho_{\text{rad}}(t_{\text{wd}})$, thus

$$\rho_{\text{wall}}(t_{\text{ann}}) = \frac{t_{\text{wd}}}{t_{\text{ann}}} \rho_{\text{rad}}(t_{\text{wd}}) = \frac{H(T_{\text{ann}})}{H(T_{\text{wd}})} \rho_{\text{rad}}(t_{\text{wd}}). \quad (3.18)$$

Assuming radiation domination up to this point, the wall-domination temperature T_{wd} is

$$T_{\text{wd}} \simeq \frac{0.9 \times 10^{-9} \text{ GeV}}{[g_\star(T_{\text{wd}})]^{1/4}} \left(\frac{\sigma}{\text{GeV}^3}\right)^{1/2} \simeq \frac{2.0 \text{ GeV} [g_\star(T_\star)]^{1/2}}{[g_\star(T_{\text{wd}})g_\star(T_{\text{ann}})]^{1/4}} \left(\frac{T_\star}{\text{GeV}}\right)^2 \left(\frac{\text{GeV}}{T_{\text{ann}}}\right), \quad (3.19)$$

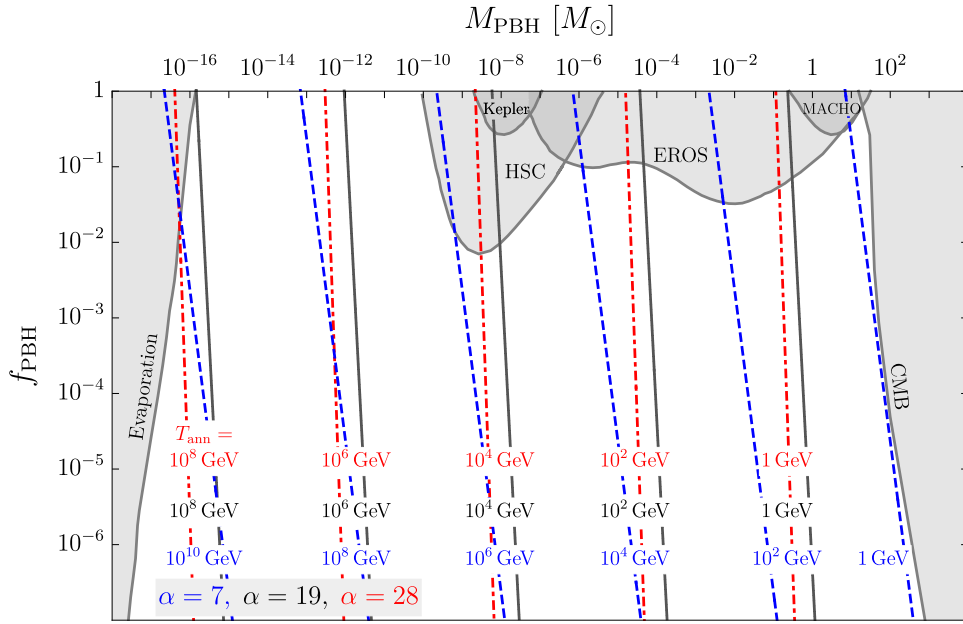


Figure 1. Fraction of the DM in PBH as a function of the PBH mass (assuming a monochromatic mass function) for different values of the string-wall system annihilation temperature T_{ann} (see eq. (3.23)) and of the parameter α (7 for dashed blue lines, 19 for solid gray lines and 28 for dash dotted red lines). Observational upper limits on f_{PBH} are shown in gray (see main text for details).

or

$$T_{\text{wd}} \simeq \frac{3.4 \text{ GeV}}{[g_{\star}(T_{\text{wd}})]^{1/4}} \frac{f_{\sigma}^{1/2}}{N} \left(\frac{V}{10^9 \text{ GeV}} \right) \left(\frac{m_a}{10 \text{ GeV}} \right)^{1/2}. \quad (3.20)$$

Considering the redshift of the radiation density to the present, eq. (3.17) becomes

$$f_{\text{PBH}} \simeq \frac{g_{s\star}(T_0)}{g_{\star}(T_0)} \frac{[g_{\star}(T_{\text{ann}})g_{\star}(T_{\text{wd}})]^{1/2}}{g_{s\star}(T_{\star})} \frac{T_{\star}^{(\alpha-3)} T_{\text{wd}}^2}{T_0 T_{\text{ann}}^{(\alpha-2)}} \left(\frac{\rho_{\text{rad}}}{\rho_{\text{DM}}}_0 \right), \quad (3.21)$$

or, using eq. (3.19),

$$f_{\text{PBH}} \simeq \frac{4.0 g_{s\star}(T_0)}{g_{\star}(T_0)} \frac{g_{\star}(T_{\star})}{g_{s\star}(T_{\star})} \frac{T_{\star}^{(\alpha+1)}}{T_0 T_{\text{ann}}^{\alpha}} \left(\frac{\rho_{\text{rad}}}{\rho_{\text{DM}}}_0 \right). \quad (3.22)$$

Using eq. (3.10) and the values of the present quantities in the previous equation we find

$$f_{\text{PBH}} \simeq 1.1 \times 10^{14} \times 1.5^{\alpha} \times 10^{-2\alpha} \left(\frac{10^{-10} M_{\odot}}{M_{\text{PBH}}} \right)^{(\alpha+1)/2} \left(\frac{10^6 \text{ GeV}}{T_{\text{ann}}} \right)^{\alpha} \times \left(\frac{105}{g_{\star}(T_{\star})} \right)^{(\alpha-3)/4} \left(\frac{105}{g_{s\star}(T_{\star})} \right). \quad (3.23)$$

In the following we neglect the possible change of energy degrees of freedom between T_{ann} and T_{\star} , since these temperatures are always close to each other.

Figure 1 shows upper limits on the fraction of DM in PBH f_{PBH} as a function of the PBH mass M_{PBH} . The constraints correspond to Hawking's evaporation bounds [9, 12, 13, 107–110], microlensing bounds [15, 16, 33, 111, 112], and CMB bounds [113]. All bounds on

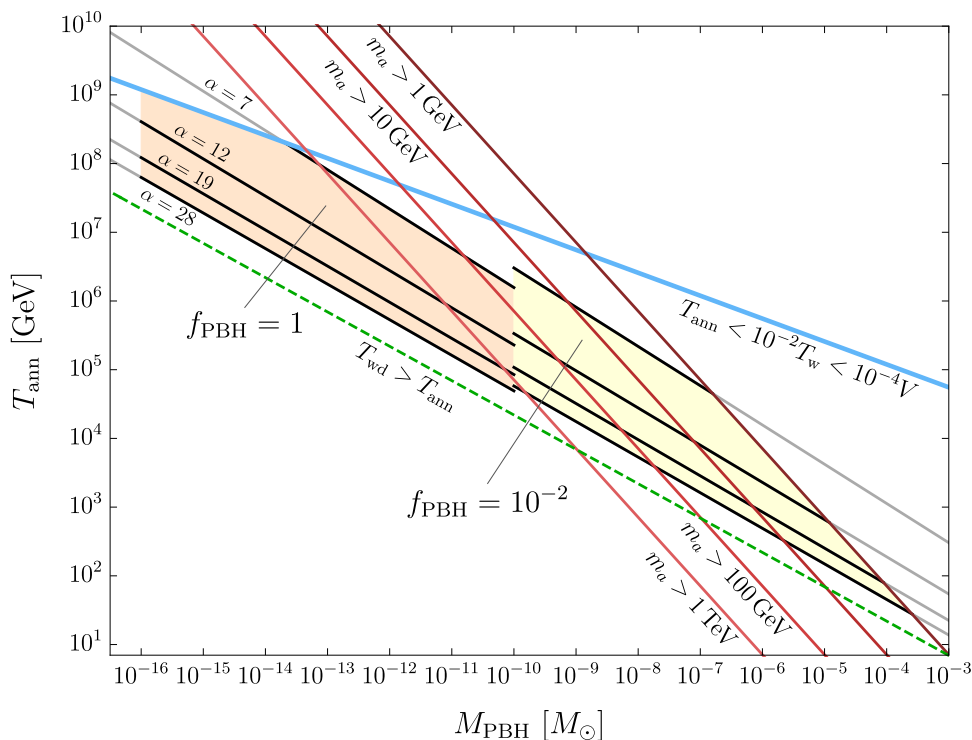


Figure 2. Range of T_{ann} as function of PBH mass for which eq. (3.23) implies that PBHs can account for all of the DM, i.e. $f_{\text{PBH}} = 1$ (orange band) or $f_{\text{PBH}} = 10^{-2}$ (yellow band) which is allowed by all upper limits (as shown in figure 1). Each lower limit on m_a excludes the region above and to the right of the corresponding red line, imposing for consistency of the model that $T_w < 10^{-2} V$ (i.e. m_a can only be larger than the quoted limit to the left of the lines, and can be both smaller on both sides). Other consistency conditions, $T_{\text{ann}} < 10^{-2} T_w < 10^{-4} V$ and $T_{\text{wd}} < T_{\text{ann}}$, reject the regions above the thick blue line and below the dashed green line, respectively.

the PBH abundance are taken from ref. [18], except for the ones from the Subaru Hyper Suprime-Cam (HSC) data [16, 33]. Additional constraints, independent of cosmology, relies on dwarf galaxy heating [114, 115]. The parameter space will be further probed by upcoming experiments [116, 117]. The lines of constant annihilation temperature T_{ann} implied by eq. (3.23) for different values of the parameter α are shown in dashed blue for $\alpha = 7$, solid gray for $\alpha = 19$ and dash dotted red for $\alpha = 28$. We can clearly see in the figure that there are annihilation temperatures, in the mass range $10^{-16} M_{\odot} < M_{\text{PBH}} < 10^{-10} M_{\odot}$, for which all of the DM could be in PBHs.

The range of T_{ann} for which PBHs can constitute 100% of the DM is better seen as the orange band in figure 2. The yellow band in the same figure shows the range of T_{ann} in which, according to eq. (3.23) $f_{\text{PBH}} = 10^{-2}$, a DM fraction that is just below all the observational bounds for $10^{-10} M_{\odot} < M_{\text{PBH}} < 1 M_{\odot}$. Such PBHs could potentially account for some putative events, as found by HSC [16] and other [15] microlensing observation, as well as LIGO observations [118].

As we explain in section 5, the consistency requirement of having walls formed well after strings appear, i.e. $T_w \ll V$, implies that a lower limit on m_a translates into a region of this plot being excluded. Assuming $T_w < 10^{-2} V$, we obtain the limits shown in figure 2 as red

lines. Each lower limit on the ALP mass (from 1 GeV to 1 TeV) excludes the region above and to the right of the corresponding red line (meaning that larger values of m_a are only possible to the left of the corresponding line, although also smaller values are possible). These limits exclude values of M_{PBH} lower than $10^{-2} M_{\odot}$ for $f_{\text{PBH}} = 10^{-2}$. Two combined consistency conditions, $T_{\text{ann}} < 10^{-2} T_{\text{w}}$ and $T_{\text{w}} < 10^{-2} V$, reject the regions above the thick blue line in figure 2. Finally, requiring the string-wall system not to dominate the energy density of the Universe, i.e. $T_{\text{wd}} < T_{\text{ann}}$, rejects the region below the dashed green line, thus it does not affect any of our regions of interest.

Notice that the some of the above mentioned consistency conditions depend on T_{w} , and thus on m_a . Therefore, they might be affected by a temperature dependence of m_a which we have neglected. However, the results depending only on the string-wall system annihilation, i.e. the present density of PBHs and GWs due to catastrophogenesis, are independent of this assumption.

4 Potentially observable GWs

Since the GWs due to the string-wall system and PBHs are produced at annihilation, their present abundance depends only on two parameters, V_{bias} and σ , which determine when annihilation happens. It is convenient here to choose the two independent parameters to be instead the GW peak frequency f_{peak} (which depends only on T_{ann} through eq. (2.10)) and the fraction of DM in PBHs, f_{PBH} , and write Ω_{GW} as

$$\Omega_{\text{GW}} h^2 \simeq \left(7.6 \times 10^{-5}\right)^{\alpha/(\alpha+1)} \left(1.4 \times 10^{-7}\right)^{20/(\alpha+1)} \left(\frac{1 \text{ Hz}}{f_{\text{peak}}} f_{\text{PBH}}\right)^{8/(\alpha+1)} \quad (4.1)$$

$$\times \left[\frac{105}{g_{\star}(T_{\text{ann}})} \left(\frac{g_{\star}(T_{\star})}{105}\right)^2\right]^{(\alpha-3)/(\alpha+1)} \left(\frac{105}{g_{s\star}(T_{\text{ann}})}\right)^{4(\alpha+3)/3(\alpha+1)} \left(\frac{g_{s\star}(T_{\star})}{105}\right)^{8/\alpha+1} .$$

Figure 3 shows the expected present GW density produced by the string-wall system as a function of f_{peak} (lower abscissa axis) or T_{ann} (upper abscissa axis). The region where PBHs can be all of the DM ($f_{\text{PBH}} = 1$) and the one where they can constitute only a DM subcomponent ($f_{\text{PBH}} = 10^{-2}$) are shown respectively in orange and yellow. We consider a range of α values, 7 to 28 (black solid lines). The predictions are compared to the current upper limits (solid contours) and the expected reach (dashed contours) of several GW detectors. We include the projected sensitivities of the space-based experiments TianQin [119], Taiji [120], and the Laser Interferometer Space Antenna (LISA) [121] in green, the reach of the Atom Interferometer Observatory and Network (AION) [122], the Atomic Experiment for Dark Matter and Gravity Exploration in Space (AEDGE) [123], the Deci-hertz Interferometer Gravitational wave Observatory (DECIGO) [124], and the Big Bang Observer (BBO) [125] in blue. Finally, we show in red the reach of the ground based experiments Einstein Telescope (ET) (projection) [103] and in grey limits and future reach of the Laser Interferometer Gravitational-Wave Observatory (LIGO) [126]. The cyan band corresponds to the 95% C.L. upper limit on the effective number of degrees of freedom during CMB emission from Planck, and other data [127], which imposes $\Omega_{\text{GW}} h^2 < 10^{-6}$.

Also shown in figure 3 are the dotted gray lines of constant PBH mass, from 10^{-16} to $10^{-4} M_{\odot}$, stemming from the following relation,

$$\Omega_{\text{GW}} h^2 \simeq 1.4 \times 10^{-9} \frac{105 [g_{\star}(T_{\text{ann}})]^3}{[g_{s\star}(T_{\text{ann}})]^4} \left(\frac{M_{\odot}}{M_{\text{PBH}}}\right)^4 \left(\frac{10^{-7} \text{ Hz}}{f_{\text{peak}}}\right)^8 . \quad (4.2)$$

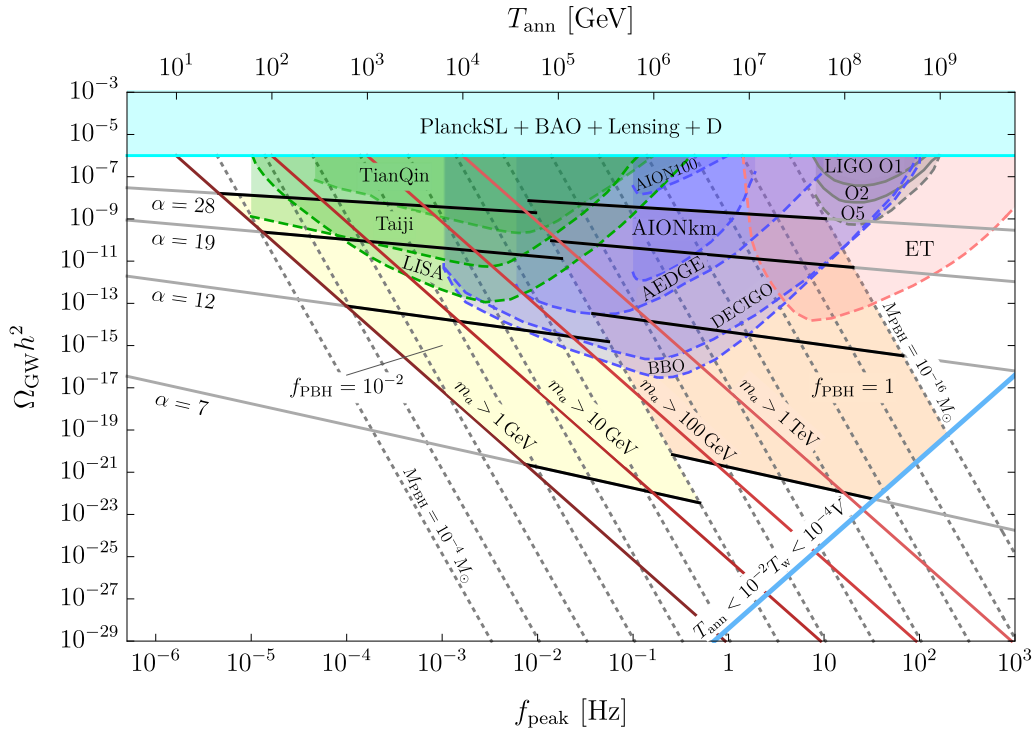


Figure 3. Present GW density $\Omega_{\text{GW}} h^2$ emitted by the string-wall system predominantly at annihilation, as a function of f_{peak} (lower abscissa axis) or T_{ann} (upper abscissa axis) for $f_{\text{PBH}} = 1$ (orange region) or $f_{\text{PBH}} = 10^{-2}$ (yellow region) expected for different values of the power index α , between 7 and 28 (solid black lines). We also show upper limits (solid contours) and the expected reach (dashed contours) of existing and future GW detectors, respectively. The quoted lower limits on m_a allow only the regions above and to the right of the respective slanted red lines (meaning that m_a can be larger than the quoted values only to the right side of the lines, and can be smaller on both sides) if $T_w/V = 10^{-2}$ (for smaller values of this ratio the allowed regions shrink). Gray dotted lines indicate constant PBH mass values. The consistency condition $T_{\text{ann}} < 10^{-2} T_w < 10^{-4} V$ rejects the region below and to the right of the thick blue line.

As explained in the next section, the lower limits quoted on the ALP mass (between 1 GeV and 1 TeV) allow only the regions above and to the right of the respective slanted red lines (meaning that m_a cannot be larger than the quoted limit to the left) if $T_w/V = 10^{-2}$. For smaller values of the T_w/V ratio the allowed regions shrink, i.e. the slanted red lines move to the right.

Figure 3 clearly demonstrates that a GW signal due to the annihilation of the cosmic walls is within the reach of several experiments for values of α above about 12, both if PBHs constitute the whole of the DM or just a small fraction of it.

Contrary to the GW signal from wall annihilation, the GW signal emitted by strings before walls appear depends on the ALP mass value. Therefore, we do not show the signal from strings in figure 3. Eq. (2.14) shows that for $m_a > 1 \text{ GeV}$ strings contribute to the GW predicted spectrum only above $f_{\text{cut}}^{\text{st}} = 82 \text{ Hz}$, and the cutoff frequency moves rapidly to higher frequencies as $m_a^{1/2}$, moving from LIGO frequency range to the range which will be probed by ET. However, eq. (2.12) shows that the GW energy density due to cosmic strings is always

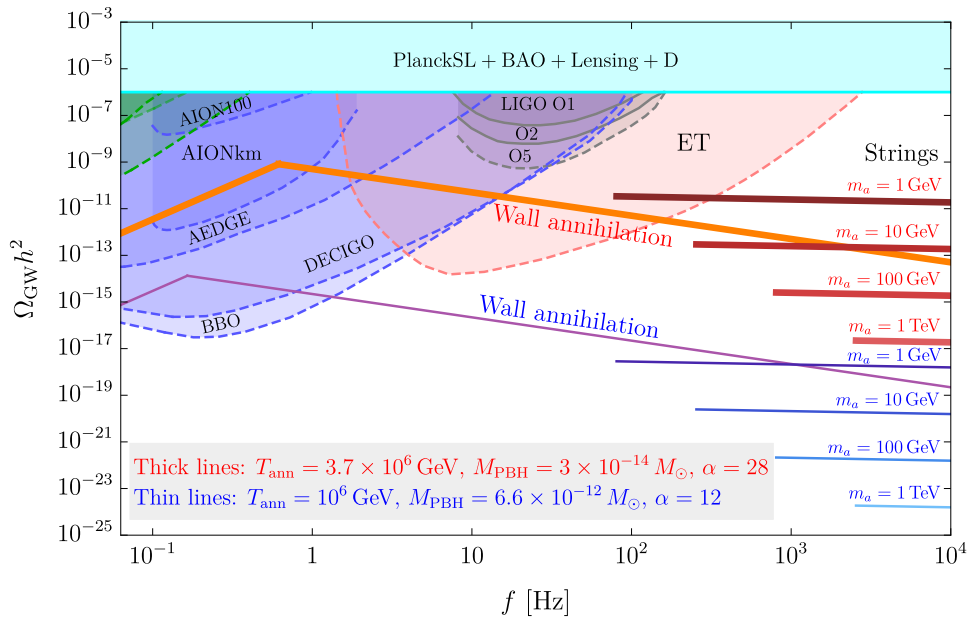


Figure 4. Two examples of combined GW spectra from wall annihilation and from string emission: for a model with $\alpha = 28$ the spectrum from wall annihilation (thick red solid lines) is observable in several future GW detectors, and the corresponding spectrum from strings (thick dark red lines) for the m_a values indicated would be observable by ET only for $m_a \simeq 1$ GeV; for a more typical example of a model with lower α value, $\alpha = 12$, the GWs from wall annihilation (in violet) are observable, but the corresponding spectrum from strings (in blue) is not observable.

below 10^{-9} , since we only consider $V < 10^{16}$ GeV, thus putting the signal out of the reach of LIGO. The signal is potentially within the reach of ET only for models with very large values of α . Figure 4 shows two examples of GW spectra from wall annihilation and from string emission. One of them with $\alpha = 28$ has a large peak amplitude from wall annihilation, with a spectrum $\sim f^3$ below the peak and $\sim 1/f$ above it (thick red lines), that would be largely observable in several future GW detectors. The corresponding spectrum from strings, shown in dark red for several values of m_a , would be observable by ET only for $m_a \simeq 1$ GeV. The other spectra correspond to more typical examples with lower value of α , $\alpha = 12$. In this case the GWs from wall annihilation (shown in violet) could still be observed by DECIGO and BBO, but the GWs from strings (in blue, each for the indicated m_a value) could not.

Similar predictions for GWs from wall annihilation were found in ref. [93] for the high-quality QCD axion model. Because our consistency conditions are tighter and we include the production of asteroid-mass PBHs, we find a less prominent GW signal. Assuming for example $\alpha = 7$, we find that above 1 Hz the GW amplitude cannot be larger than $\Omega_{\text{GW}} h^2 \simeq 10^{-19}$.

5 Self consistency conditions

Consistency of our models requires that the annihilation of the string-wall system happens before walls would become dominant in the Universe and well after the formation of domain walls, which in turn appear sufficiently after the formation of the cosmic string network, i.e. that 10^{16} GeV $> V \gg T_w \gg T_{\text{ann}} > T_{\text{wd}}$. Conservatively, we will require $T_w/V \lesssim 10^{-2}$ and $T_{\text{ann}}/T_w \lesssim 10^{-2}$ as well.

Our model has three independent parameters, which at the level of the Lagrangian are V , $v \ll V$, and $\epsilon_b \ll 1$. Instead of v , we could alternatively use m_a through eq. (2.2), with $m_a \ll V$. But for our problem it is convenient to choose as the independent parameters T_{ann} and M_{PBH} (on which anything dependent only on the annihilation depends), as well as m_a . In terms of these parameters,

$$V \simeq \frac{3}{16\pi} \left(\frac{10}{\pi}\right)^{1/4} \frac{NM_{\text{P}}^{7/2}}{f_\sigma^{1/2} [g_\star(T_{\text{ann}})]^{1/4} m_a^{1/2} T_{\text{ann}} M_{\text{PBH}}}, \quad (5.1)$$

or

$$V \simeq 1.4 \times 10^{12} \text{ GeV} \frac{N}{f_\sigma^{1/2}} \left(\frac{105}{g_\star(T_{\text{ann}})}\right)^{1/4} \left(\frac{1 \text{ GeV}}{m_a}\right)^{1/2} \left(\frac{10^6 \text{ GeV}}{T_{\text{ann}}}\right) \left(\frac{10^{-10} M_\odot}{M_{\text{PBH}}}\right), \quad (5.2)$$

and

$$\epsilon_b = 1.2 \times 10^{-5} \left(\frac{g_\star(T_{\text{ann}})}{105}\right)^{1/2} \left(\frac{T_{\text{ann}}}{10^6 \text{ GeV}}\right)^2 \left(\frac{1 \text{ GeV}}{m_a}\right). \quad (5.3)$$

As shown in eq. (2.4), T_{w} depends only on m_a , since walls appear when $H(T_{\text{w}}) \simeq m_a/3$. Extracting m_a from the ratio T_{w}/V we can write

$$m_a \simeq 29 \text{ GeV} \frac{(T_{\text{w}}/V)}{10^{-2}} \frac{N}{f_\sigma^{1/2}} \left(\frac{g_\star(T_{\text{w}})}{g_\star(T_{\text{ann}})}\right)^{1/4} \left(\frac{10^6 \text{ GeV}}{T_{\text{ann}}}\right) \left(\frac{10^{-10} M_\odot}{M_{\text{PBH}}}\right) \quad (5.4)$$

from which a lower limit on m_a , for a fixed T_{w}/V , imposes a limit in the $T_{\text{ann}}, M_{\text{PBH}}$ plane. The limits so derived are shown as red lines (for m_a larger than 1 GeV, 10 GeV, 100 GeV and 1 TeV) for $T_{\text{w}}/V = 10^{-2}$ in figure 2, where they reject the region above and to the right of the lines, and in figure 3, where they reject the region below and to the left of the lines. As T_{w}/V decreases, the limits become stronger, rejecting larger regions of the parameter space.

Notice that using eq. (2.5), when $T \simeq V$ and strings appear

$$H(V) = 1.4 \times 10^{-2} \left[\frac{V}{10^{16} \text{ GeV}}\right] V \left[\frac{g_\star(V)}{105}\right]^{1/2}, \quad (5.5)$$

and requiring $H(T_{\text{w}}) < H(V)$, i.e. that walls appear sufficiently after strings, implies

$$m_a < 4.2 \times 10^{-2} \left[\frac{V}{10^{16} \text{ GeV}}\right] V \left[\frac{g_\star(V)}{105}\right]^{1/2} < 4.2 \times 10^{-2} V \left[\frac{g_\star(V)}{105}\right]^{1/2}. \quad (5.6)$$

This shows that the upper limit due to inflation $V < 10^{16} \text{ GeV}$ already implies that $m_a \lesssim 10^{-2} V$.

Using eq. (2.8), we can easily see that the Hubble parameter at annihilation is $H(T_{\text{ann}}) = \epsilon_b m_a / (\sqrt{2} f_\sigma) = \epsilon_b m_a / 8.46$ (recall that we use $f_\sigma = 6$). Thus the condition for annihilation to happen sufficiently after walls appear, i.e. $H(T_{\text{ann}})/H(T_{\text{w}}) \ll 1$, is equivalent to requiring a small enough ϵ_b value. Notice that since $H(T_{\text{w}}) \simeq m_a/3$ and $H(T_{\text{ann}})/H(T_{\text{w}}) = (T_{\text{ann}}/T_{\text{w}})^2$,

$$\epsilon_b = 2.8 \left(\frac{T_{\text{ann}}}{T_{\text{w}}}\right)^2. \quad (5.7)$$

Thus having ϵ_b small enough is the same as having $T_{\text{ann}} \ll T_{\text{w}}$.

Extracting m_a from the ratio T_{ann}/T_w one gets,

$$m_a \simeq 4.2 \times 10^{-2} \text{ GeV} \left(\frac{10^{-2}}{T_{\text{ann}}/T_w} \right)^2 \left(\frac{g_*(T_w)}{105} \right)^{1/2} \left(\frac{T_{\text{ann}}}{10^6 \text{ GeV}} \right)^2, \quad (5.8)$$

and equating this expression for m_a with that in eq. (5.4), we obtain a relation which does not contain m_a and can be written as

$$\frac{T_{\text{ann}}}{10^6 \text{ GeV}} \simeq 8.9 \frac{N^{1/3}}{f_\sigma^{1/6}} \left(\frac{105}{g_*(T_w)} \frac{105}{g_*(T_{\text{ann}})} \right)^{1/12} \left(\frac{10^{-10} M_\odot}{M_{\text{PBH}}} \right)^{1/3} \left(\frac{T_w/V}{10^{-2}} \right)^{2/3} \left(\frac{T_{\text{ann}}/T_w}{10^{-2}} \right)^{1/3}. \quad (5.9)$$

Thus, requiring $T_w/V < 10^{-2}$ and $T_{\text{ann}}/T_w < 10^{-2}$, this last expression imposes an M_{PBH} dependent upper limit on T_{ann} shown as the blue thick line in figure 2 and figure 3.

Finally, let us ensure that wall-domination never happens before annihilation. Had the walls not annihilated previously, the walls would dominate over radiation when $\sigma/t_{\text{wd}} \simeq \rho(T_{\text{wd}})$ or

$$H(T_{\text{wd}}) = \frac{16\pi}{3} \frac{\sqrt{2}f_\sigma}{N^2} \left(\frac{V}{M_{\text{P}}} \right)^2 m_a \simeq 2.7 \times 10^{-6} \left(\frac{V}{10^{16} \text{ GeV}} \right)^2 m_a. \quad (5.10)$$

Thus, $H(T_{\text{wd}}) < H(T_{\text{ann}}) \simeq 0.33 (T_{\text{ann}}/T_w)^2 m_a$ means that

$$\frac{V}{10^{16} \text{ GeV}} < 3.5 \times 10^2 \left(\frac{T_{\text{ann}}}{T_w} \right). \quad (5.11)$$

This condition is automatically fulfilled for $T_{\text{ann}}/T_w = 10^{-2}$ since we require $V < 10^{16} \text{ GeV}$. For smaller values of this ratio we check now that eq. (5.11) is fulfilled. In terms of temperatures this condition is

$$\frac{T_{\text{wd}}}{T_{\text{ann}}} \simeq 4.8 \times 10^{-4} \left(\frac{105}{g_*(T_{\text{ann}})} \right)^{1/4} \left(\frac{105}{g_*(T_{\text{wd}})} \right)^{1/4} \left(\frac{10^6 \text{ GeV}}{T_{\text{ann}}} \right)^2 \left(\frac{10^{-10} M_\odot}{M_{\text{PBH}}} \right) < 1. \quad (5.12)$$

This limit rejects the region below and to the left of the dashed green line in figure 2, and thus does not constrain our regions of interest.

6 Concluding remarks

Many extensions of the Standard Model of particle physics feature U(1) symmetries whose breaking is associated with the existence of heavy pGBs. There are QCD axion, ALP, and majoron models of this type. If the pGBs are unstable and decay in the early Universe, they cannot constitute the DM, and thus such models might lack a particle DM candidate.

Potentials which admit a number $N > 1$ of minima along the orbit of vacua imply the formation of a string-wall network whose annihilation is accompanied by catastogenesis [34], i.e. the production of GWs, pGBs, and PBHs. We find that for annihilation temperatures $10^4 \text{ GeV} \lesssim T_{\text{ann}} \lesssim 10^9 \text{ GeV}$, one can form asteroid-mass PBHs ($10^{-16} M_\odot \lesssim M_{\text{PBH}} \lesssim 10^{-10} M_\odot$) that can constitute the entirety of the dark matter. For slightly smaller annihilation temperatures, $1 \text{ GeV} \lesssim T_{\text{ann}} \lesssim 10^5 \text{ GeV}$, the PBHs produced have mass $10^{-10} M_\odot \lesssim M_{\text{PBH}} \lesssim 10 M_\odot$, and could potentially account for HSC [16] and other [15] microlensing observations, and they can account for part of the mergers observed by LIGO [118]. The resulting PBH masses depend on α , an exponent that parameterizes the annihilation rate of the string-wall network and needs to be determined from simulations of this process.

The GW signal produced by catastrogenesis together with PBHs can have an amplitude as large as $\Omega_{\text{GW}}h^2 \simeq 10^{-7}$ and can be observable in future GW detectors. For a particularly favorable set of parameters, the GWs emitted from strings alone, before walls appear, could be observable as well.

Notice that although in this paper we do not study the breaking of purely discrete symmetries, in principle our mechanism also applies to this case. The main ingredient is the existence of multiple vacua. Therefore, the breaking of a discrete symmetry can also result in a scenario similar to the one described here, as far as the wall system annihilates mostly into unstable particles, such as flavons [86], whose decay products thermalize.

There are several caveats concerning the interpretation of our results. The production of PBHs relies on the formation of closed domain walls which must retain a high degree of sphericity during the last stages of their collapse. The amplitude of the stochastic GW background produced by catastrogenesis is delicately sensitive to the precise evolution of the string-wall network at the very end of its existence. Clarifying both these issues requires dedicated simulations of the process of annihilation of the network, which we hope will be tackled in the future. The collapse of string-wall networks associated with heavy ALPs is an open problem worth examining in further detail.

Acknowledgments

The work of GG was supported in part by the U.S. Department of Energy (DOE) Grant No. DE-SC0009937. EV acknowledges support by the European Research Council (ERC) under the European Union's Horizon Europe research and innovation programme (grant agreement No. 101040019). Views and opinions expressed are however those of the author(s) only and do not necessarily reflect those of the European Union.

A Brief derivation of the present GW energy density

The estimate of the power P emitted in GWs is obtained from the quadrupole formula $P \simeq G\ddot{Q}_{ij}\ddot{Q}_{ij}$ [99]. The energy in the walls in the scaling regime is $E_w \simeq \sigma t^2$, thus the quadrupole moment of the walls is $Q_{ij} \simeq E_w t^2$ and $\ddot{Q}_{ij} \simeq \sigma t$. Therefore $P \simeq G\sigma^2 t^2$. The energy density $\Delta\rho_{\text{GW}}$ emitted by the string-wall system in a time interval Δt is then $\Delta\rho_{\text{GW}}(t) \simeq P\Delta t/t^3 \simeq G\sigma^2\Delta t/t$. Thus, in a time interval equal to the Hubble time $\Delta t \simeq t$, $\Delta\rho_{\text{GW}}(t) \simeq G\sigma^2$ independently of the emission time t . This energy density is redshifted so its contribution to the present-day GW energy density is $\Delta\rho_{\text{GW}}(t)(R(t)/R_0)^4 \simeq G\sigma^2(R(t)/R_0)^4$, where $R(t)$ and $R_0 = 1$ are the scale factors of the Universe at time t and at present.

This argument clearly shows that the largest contribution to the present GW energy density spectrum emitted by the string-wall network, i.e. its peak amplitude, corresponds to the latest emission time, $t \simeq t_{\text{ann}}$, i.e. $\rho_{\text{GW}}|_{\text{peak}} \simeq G\sigma^2(R(t_{\text{ann}})/R_0)^4$. Defining as usual $\Omega_{\text{GW}}h^2|_{\text{peak}} = \rho_{\text{GW}}|_{\text{peak}}(h^2/\rho_c)$, this leads to eq. (2.11). Here ρ_c is the present critical density, h is the reduced Hubble constant, and entropy conservation implies that $g_{s*}(t)[R(t)T(t)]^3$ is constant, and at present the number of entropy degrees of freedom is $g_{s*}(t_0) \simeq 3.93$ [90].

What is usually quoted is the maximum of the GW energy density spectrum at time t as a function of the wave-number at present k , which for $R_0 = 1$ coincides with the comoving wave-number (or the frequency $f = k/(2\pi)$), defined as

$$\Omega_{\text{GW}}h^2(k, t) = \left(\frac{h^2}{\rho_c(t)} \right) \left(\frac{d\rho_{\text{GW}}(t)}{d \ln k} \right), \quad (\text{A.1})$$

(see e.g. refs. [86, 99]). This is also given by eq. (2.11), since

$$\frac{d\rho_{\text{GW}}(t)}{d\ln(k)} \simeq G\sigma^2 \quad (\text{A.2})$$

independently of t . This is so because in the scaling regime the characteristic frequency of the GWs emitted at t is $\simeq H(t)$ (the inverse of the horizon size). Thus the present-day frequency of GWs emitted at time t is $f \simeq R(t)H(t)$. For GWs emitted in the radiation dominated epoch, when $H(t) = (2t)^{-1}$, $d\ln f = (H(t) - t^{-1})dt$, and $d\ln f = d\ln k = -(1/2) d\ln t$. Using from above that $d\rho_{\text{GW}}(t) \simeq G\sigma^2(dt/t) = G\sigma^2 d\ln(t)$, we find eq. (A.2). Thus the peak amplitude of this GW spectrum at present, for $t = t_0$, coincides with the result in eq. (2.11). Since the peak GW density of walls is emitted at annihilation, its present frequency is $f_{\text{peak}} \simeq R(t_{\text{ann}})H(t_{\text{ann}})$, as given in eq. (2.10).

The spectrum of the GWs emitted by cosmic walls cannot be determined from the previous considerations alone, but has been computed numerically for $N > 1$ in ref. [98]. Figure 6 of ref. [98] shows that there is a peak at $k|_{\text{peak}} \simeq R(t_f)m_a$, a bump at the scale $k \simeq R(t_f)H(t_f)$ where t_f is the latest time in their simulation, and the spectral slope changes at these two scales. Causality requires that for frequencies below the peak, $k < k_{\text{peak}}$ corresponding to super-horizon wavelengths at t_{ann} , the spectrum goes as k^3 . This is a white noise spectrum characteristic of the absence of causal correlations [128]. At frequencies above the peak, $k > k_{\text{peak}}$, the spectrum depends instead on the particular GW production model assumed. The spectrum $1/k$ was found analytically for a source that is not correlated at different times, i.e. that consists of a series of short events [128] (see also ref. [129]). Ref. [98] obtained roughly a $1/k$ spectrum for $k > k_{\text{peak}}$, with approximate slope and height of the secondary bump that depend on N .

Similarly to what is done for the string-wall system, the estimates of the GW density emitted by the string network before walls appear are based on the quadrupole formula (see e.g. refs. [100–102] and references therein). The energy of the string network is $E_{\text{st}} \simeq \mu H^{-1}$, where μ is the string mass per unit length. Thus $\ddot{Q}_{ij} \simeq \mu$, and the power emitted in GWs is $P \simeq G\mu^2$. Using the same assumptions as for the walls, the energy density $\Delta\rho_{\text{GW}}$ for strings is $\Delta\rho_{\text{GW}}^{\text{st}}(t) \simeq G\mu^2(\Delta t)$. The resulting spectrum has been computed in refs. [100–102], and the simple expression in eq. (2.12) provides a good fit to all of them, for frequencies $f > f_{\text{cut}}^{\text{st}}$. The cutoff frequency $f_{\text{cut}}^{\text{st}}$ in eq. (2.14) corresponds to the frequency emitted at T_w when walls appear and the string network ceases to exist.

References

- [1] G. Bertone, D. Hooper and J. Silk, *Particle dark matter: Evidence, candidates and constraints*, *Phys. Rept.* **405** (2005) 279 [[hep-ph/0404175](#)] [[INSPIRE](#)].
- [2] J. de Swart, G. Bertone and J. van Dongen, *How Dark Matter Came to Matter*, *Nature Astron.* **1** (2017) 0059 [[arXiv:1703.00013](#)] [[INSPIRE](#)].
- [3] Y.B. Zel’dovich and I.D. Novikov, *The Hypothesis of Cores Retarded during Expansion and the Hot Cosmological Model*, *Sov. Astron.* **10** (1967) 602.
- [4] S. Hawking, *Gravitationally collapsed objects of very low mass*, *Mon. Not. Roy. Astron. Soc.* **152** (1971) 75 [[INSPIRE](#)].
- [5] B.J. Carr and S.W. Hawking, *Black holes in the early Universe*, *Mon. Not. Roy. Astron. Soc.* **168** (1974) 399 [[INSPIRE](#)].

- [6] B.J. Carr, *The primordial black hole mass spectrum*, *Astrophys. J.* **201** (1975) 1 [INSPIRE].
- [7] B. Carr, K. Kohri, Y. Sendouda and J. Yokoyama, *Constraints on primordial black holes*, *Rept. Prog. Phys.* **84** (2021) 116902 [arXiv:2002.12778] [INSPIRE].
- [8] B. Carr and F. Kuhnel, *Primordial black holes as dark matter candidates*, *SciPost Phys. Lect. Notes* **48** (2022) 1 [arXiv:2110.02821] [INSPIRE].
- [9] B.J. Carr, K. Kohri, Y. Sendouda and J. Yokoyama, *New cosmological constraints on primordial black holes*, *Phys. Rev. D* **81** (2010) 104019 [arXiv:0912.5297] [INSPIRE].
- [10] S.W. Hawking, *Black hole explosions*, *Nature* **248** (1974) 30 [INSPIRE].
- [11] S.W. Hawking, *Particle Creation by Black Holes*, *Commun. Math. Phys.* **43** (1975) 199 [Erratum *ibid.* **46** (1976) 206] [INSPIRE].
- [12] M. Boudaud and M. Cirelli, *Voyager 1 e^\pm Further Constrain Primordial Black Holes as Dark Matter*, *Phys. Rev. Lett.* **122** (2019) 041104 [arXiv:1807.03075] [INSPIRE].
- [13] W. DeRocco and P.W. Graham, *Constraining Primordial Black Hole Abundance with the Galactic 511 keV Line*, *Phys. Rev. Lett.* **123** (2019) 251102 [arXiv:1906.07740] [INSPIRE].
- [14] A. Coogan, L. Morrison and S. Profumo, *Direct Detection of Hawking Radiation from Asteroid-Mass Primordial Black Holes*, *Phys. Rev. Lett.* **126** (2021) 171101 [arXiv:2010.04797] [INSPIRE].
- [15] EROS-2 collaboration, *Limits on the Macho Content of the Galactic Halo from the EROS-2 Survey of the Magellanic Clouds*, *Astron. Astrophys.* **469** (2007) 387 [astro-ph/0607207] [INSPIRE].
- [16] H. Niikura et al., *Microlensing constraints on primordial black holes with Subaru/HSC Andromeda observations*, *Nature Astron.* **3** (2019) 524 [arXiv:1701.02151] [INSPIRE].
- [17] H. Niikura et al., *Constraints on Earth-mass primordial black holes from OGLE 5-year microlensing events*, *Phys. Rev. D* **99** (2019) 083503 [arXiv:1901.07120] [INSPIRE].
- [18] B.J. Kavanagh, *bradkav/PBHbounds*, <https://github.com/bradkav/PBHbounds> [DOI:10.5281/ZENODO.3538999].
- [19] J. Yokoyama, *Formation of MACHO primordial black holes in inflationary cosmology*, *Astron. Astrophys.* **318** (1997) 673 [astro-ph/9509027] [INSPIRE].
- [20] J. Garcia-Bellido, A.D. Linde and D. Wands, *Density perturbations and black hole formation in hybrid inflation*, *Phys. Rev. D* **54** (1996) 6040 [astro-ph/9605094] [INSPIRE].
- [21] G. Ballesteros and M. Taoso, *Primordial black hole dark matter from single field inflation*, *Phys. Rev. D* **97** (2018) 023501 [arXiv:1709.05565] [INSPIRE].
- [22] S.W. Hawking, I.G. Moss and J.M. Stewart, *Bubble Collisions in the Very Early Universe*, *Phys. Rev. D* **26** (1982) 2681 [INSPIRE].
- [23] M. Lewicki and V. Vaskonen, *On bubble collisions in strongly supercooled phase transitions*, *Phys. Dark Univ.* **30** (2020) 100672 [arXiv:1912.00997] [INSPIRE].
- [24] S.W. Hawking, *Black Holes From Cosmic Strings*, *Phys. Lett. B* **231** (1989) 237 [INSPIRE].
- [25] M. Khlopov, B.A. Malomed and I.B. Zeldovich, *Gravitational instability of scalar fields and formation of primordial black holes*, *Mon. Not. Roy. Astron. Soc.* **215** (1985) 575 [INSPIRE].
- [26] E. Cotner and A. Kusenko, *Primordial black holes from supersymmetry in the early universe*, *Phys. Rev. Lett.* **119** (2017) 031103 [arXiv:1612.02529] [INSPIRE].
- [27] E. Cotner, A. Kusenko and V. Takhistov, *Primordial Black Holes from Inflaton Fragmentation into Oscillons*, *Phys. Rev. D* **98** (2018) 083513 [arXiv:1801.03321] [INSPIRE].

- [28] E. Cotner, A. Kusenko, M. Sasaki and V. Takhistov, *Analytic Description of Primordial Black Hole Formation from Scalar Field Fragmentation*, *JCAP* **10** (2019) 077 [[arXiv:1907.10613](#)] [[INSPIRE](#)].
- [29] M.M. Flores and A. Kusenko, *Primordial Black Holes from Long-Range Scalar Forces and Scalar Radiative Cooling*, *Phys. Rev. Lett.* **126** (2021) 041101 [[arXiv:2008.12456](#)] [[INSPIRE](#)].
- [30] J. Garriga, A. Vilenkin and J. Zhang, *Black holes and the multiverse*, *JCAP* **02** (2016) 064 [[arXiv:1512.01819](#)] [[INSPIRE](#)].
- [31] H. Deng, J. Garriga and A. Vilenkin, *Primordial black hole and wormhole formation by domain walls*, *JCAP* **04** (2017) 050 [[arXiv:1612.03753](#)] [[INSPIRE](#)].
- [32] H. Deng and A. Vilenkin, *Primordial black hole formation by vacuum bubbles*, *JCAP* **12** (2017) 044 [[arXiv:1710.02865](#)] [[INSPIRE](#)].
- [33] A. Kusenko et al., *Exploring Primordial Black Holes from the Multiverse with Optical Telescopes*, *Phys. Rev. Lett.* **125** (2020) 181304 [[arXiv:2001.09160](#)] [[INSPIRE](#)].
- [34] G.B. Gelmini, A. Simpson and E. Vitagliano, *Catastrogenesis: DM, GWs, and PBHs from ALP string-wall networks*, *JCAP* **02** (2023) 031 [[arXiv:2207.07126](#)] [[INSPIRE](#)].
- [35] R.D. Peccei and H.R. Quinn, *CP Conservation in the Presence of Instantons*, *Phys. Rev. Lett.* **38** (1977) 1440 [[INSPIRE](#)].
- [36] S. Weinberg, *A New Light Boson?*, *Phys. Rev. Lett.* **40** (1978) 223 [[INSPIRE](#)].
- [37] F. Wilczek, *Problem of Strong P and T Invariance in the Presence of Instantons*, *Phys. Rev. Lett.* **40** (1978) 279 [[INSPIRE](#)].
- [38] J.E. Kim, *Weak Interaction Singlet and Strong CP Invariance*, *Phys. Rev. Lett.* **43** (1979) 103 [[INSPIRE](#)].
- [39] M.A. Shifman, A.I. Vainshtein and V.I. Zakharov, *Can Confinement Ensure Natural CP Invariance of Strong Interactions?*, *Nucl. Phys. B* **166** (1980) 493 [[INSPIRE](#)].
- [40] M. Dine, W. Fischler and M. Srednicki, *A Simple Solution to the Strong CP Problem with a Harmless Axion*, *Phys. Lett. B* **104** (1981) 199 [[INSPIRE](#)].
- [41] J. Jaeckel and A. Ringwald, *The Low-Energy Frontier of Particle Physics*, *Ann. Rev. Nucl. Part. Sci.* **60** (2010) 405 [[arXiv:1002.0329](#)] [[INSPIRE](#)].
- [42] Y. Chikashige, R.N. Mohapatra and R.D. Peccei, *Are There Real Goldstone Bosons Associated with Broken Lepton Number?*, *Phys. Lett. B* **98** (1981) 265 [[INSPIRE](#)].
- [43] I.Z. Rothstein, K.S. Babu and D. Seckel, *Planck scale symmetry breaking and majoron physics*, *Nucl. Phys. B* **403** (1993) 725 [[hep-ph/9301213](#)] [[INSPIRE](#)].
- [44] P.-H. Gu, E. Ma and U. Sarkar, *Pseudo-Majoron as Dark Matter*, *Phys. Lett. B* **690** (2010) 145 [[arXiv:1004.1919](#)] [[INSPIRE](#)].
- [45] G. Lazarides et al., *Spontaneous Breaking of Lepton Number and the Cosmological Domain Wall Problem*, *Phys. Rev. Lett.* **122** (2019) 151301 [[arXiv:1806.11198](#)] [[INSPIRE](#)].
- [46] M. Reig, J.W.F. Valle and M. Yamada, *Light majoron cold dark matter from topological defects and the formation of boson stars*, *JCAP* **09** (2019) 029 [[arXiv:1905.01287](#)] [[INSPIRE](#)].
- [47] Y. Abe et al., *TeV-scale Majorogenesis*, *JHEP* **07** (2020) 105 [[arXiv:2004.00599](#)] [[INSPIRE](#)].
- [48] S. Bansal et al., *Enhanced neutrino polarizability*, *JHEP* **05** (2023) 142 [[arXiv:2210.05706](#)] [[INSPIRE](#)].
- [49] H. Fukuda, K. Harigaya, M. Ibe and T.T. Yanagida, *Model of visible QCD axion*, *Phys. Rev. D* **92** (2015) 015021 [[arXiv:1504.06084](#)] [[INSPIRE](#)].

- [50] S. Dimopoulos, A. Hook, J. Huang and G. Marques-Tavares, *A collider observable QCD axion*, *JHEP* **11** (2016) 052 [[arXiv:1606.03097](#)] [[INSPIRE](#)].
- [51] P. Agrawal and K. Howe, *Factoring the Strong CP Problem*, *JHEP* **12** (2018) 029 [[arXiv:1710.04213](#)] [[INSPIRE](#)].
- [52] M.K. Gaillard et al., *Color unified dynamical axion*, *Eur. Phys. J. C* **78** (2018) 972 [[arXiv:1805.06465](#)] [[INSPIRE](#)].
- [53] A. Hook, S. Kumar, Z. Liu and R. Sundrum, *High Quality QCD Axion and the LHC*, *Phys. Rev. Lett.* **124** (2020) 221801 [[arXiv:1911.12364](#)] [[INSPIRE](#)].
- [54] L. Di Luzio, M. Giannotti, E. Nardi and L. Visinelli, *The landscape of QCD axion models*, *Phys. Rept.* **870** (2020) 1 [[arXiv:2003.01100](#)] [[INSPIRE](#)].
- [55] CHARM collaboration, *Search for Axion Like Particle Production in 400-GeV Proton — Copper Interactions*, *Phys. Lett. B* **157** (1985) 458 [[INSPIRE](#)].
- [56] E.M. Riordan et al., *A Search for Short Lived Axions in an Electron Beam Dump Experiment*, *Phys. Rev. Lett.* **59** (1987) 755 [[INSPIRE](#)].
- [57] M.J. Dolan et al., *Revised constraints and Belle II sensitivity for visible and invisible axion-like particles*, *JHEP* **12** (2017) 094 [Erratum *ibid.* **03** (2021) 190] [[arXiv:1709.00009](#)] [[INSPIRE](#)].
- [58] J. Blumlein et al., *Limits on neutral light scalar and pseudoscalar particles in a proton beam dump experiment*, *Z. Phys. C* **51** (1991) 341 [[INSPIRE](#)].
- [59] NA64 collaboration, *Search for Axionlike and Scalar Particles with the NA64 Experiment*, *Phys. Rev. Lett.* **125** (2020) 081801 [[arXiv:2005.02710](#)] [[INSPIRE](#)].
- [60] J. Jaeckel, P.C. Malta and J. Redondo, *Decay photons from the axionlike particles burst of type II supernovae*, *Phys. Rev. D* **98** (2018) 055032 [[arXiv:1702.02964](#)] [[INSPIRE](#)].
- [61] S. Hoof and L. Schulz, *Updated constraints on axion-like particles from temporal information in supernova SN1987A gamma-ray data*, *JCAP* **03** (2023) 054 [[arXiv:2212.09764](#)] [[INSPIRE](#)].
- [62] G. Lucente et al., *Heavy axion-like particles and core-collapse supernovae: constraints and impact on the explosion mechanism*, *JCAP* **12** (2020) 008 [[arXiv:2008.04918](#)] [[INSPIRE](#)].
- [63] A. Caputo, G. Raffelt and E. Vitagliano, *Muonic boson limits: Supernova redux*, *Phys. Rev. D* **105** (2022) 035022 [[arXiv:2109.03244](#)] [[INSPIRE](#)].
- [64] A. Caputo, H.-T. Janka, G. Raffelt and E. Vitagliano, *Low-Energy Supernovae Severely Constrain Radiative Particle Decays*, *Phys. Rev. Lett.* **128** (2022) 221103 [[arXiv:2201.09890](#)] [[INSPIRE](#)].
- [65] A. Caputo, G. Raffelt and E. Vitagliano, *Radiative transfer in stars by feebly interacting bosons*, *JCAP* **08** (2022) 045 [[arXiv:2204.11862](#)] [[INSPIRE](#)].
- [66] M. Diamond, D.F.G. Fiorillo, G. Marques-Tavares and E. Vitagliano, *Axion-sourced fireballs from supernovae*, *Phys. Rev. D* **107** (2023) 103029 [[arXiv:2303.11395](#)] [[INSPIRE](#)].
- [67] M. Diamond et al., *Multimessenger Constraints on Radiatively Decaying Axions from GW170817*, [arXiv:2305.10327](#) [[INSPIRE](#)].
- [68] D. Cadamuro and J. Redondo, *Cosmological bounds on pseudo Nambu-Goldstone bosons*, *JCAP* **02** (2012) 032 [[arXiv:1110.2895](#)] [[INSPIRE](#)].
- [69] P.F. Depta, M. Hufnagel and K. Schmidt-Hoberg, *Updated BBN constraints on electromagnetic decays of MeV-scale particles*, *JCAP* **04** (2021) 011 [[arXiv:2011.06519](#)] [[INSPIRE](#)].
- [70] S. Knapen, T. Lin, H.K. Lou and T. Melia, *Searching for Axionlike Particles with Ultraperipheral Heavy-Ion Collisions*, *Phys. Rev. Lett.* **118** (2017) 171801 [[arXiv:1607.06083](#)] [[INSPIRE](#)].

- [71] M. Bauer, M. Neubert and A. Thamm, *Collider Probes of Axion-Like Particles*, *JHEP* **12** (2017) 044 [[arXiv:1708.00443](#)] [[INSPIRE](#)].
- [72] R.Z. Ferreira, M.C.D. Marsh and E. Müller, *Strong supernovae bounds on ALPs from quantum loops*, *JCAP* **11** (2022) 057 [[arXiv:2205.07896](#)] [[INSPIRE](#)].
- [73] C. O'HARE, *cajohare/AxionLimits: AxionLimits*, <https://cajohare.github.io/AxionLimits/> [[DOI:10.5281/ZENODO.3932430](#)].
- [74] K.J. Kelly, M. Sen and Y. Zhang, *Intimate Relationship between Sterile Neutrino Dark Matter and ΔN_{eff}* , *Phys. Rev. Lett.* **127** (2021) 041101 [[arXiv:2011.02487](#)] [[INSPIRE](#)].
- [75] D.F.G. Fiorillo, G.G. Raffelt and E. Vitagliano, *Strong Supernova 1987A Constraints on Bosons Decaying to Neutrinos*, [arXiv:2209.11773](#) [[INSPIRE](#)].
- [76] J.M. Berryman, A. De Gouvêa, K.J. Kelly and Y. Zhang, *Lepton-Number-Charged Scalars and Neutrino Beamstrahlung*, *Phys. Rev. D* **97** (2018) 075030 [[arXiv:1802.00009](#)] [[INSPIRE](#)].
- [77] A. de Gouvêa et al., *Leptonic Scalars at the LHC*, *JHEP* **07** (2020) 142 [[arXiv:1910.01132](#)] [[INSPIRE](#)].
- [78] V. Brdar, M. Lindner, S. Vogl and X.-J. Xu, *Revisiting neutrino self-interaction constraints from Z and τ decays*, *Phys. Rev. D* **101** (2020) 115001 [[arXiv:2003.05339](#)] [[INSPIRE](#)].
- [79] Y.B. Zeldovich, I.Y. Kobzarev and L.B. Okun, *Cosmological Consequences of the Spontaneous Breakdown of Discrete Symmetry*, *Zh. Eksp. Teor. Fiz.* **67** (1974) 3 [[INSPIRE](#)].
- [80] A. Vilenkin, *Cosmic Strings and Domain Walls*, *Phys. Rept.* **121** (1985) 263 [[INSPIRE](#)].
- [81] P. Sikivie, *Of Axions, Domain Walls and the Early Universe*, *Phys. Rev. Lett.* **48** (1982) 1156 [[INSPIRE](#)].
- [82] S. Chang, C. Hagmann and P. Sikivie, *Axions from wall decay*, *Nucl. Phys. B Proc. Suppl.* **72** (1999) 99 [[hep-ph/9808302](#)] [[INSPIRE](#)].
- [83] G.B. Gelmini, M. Gleiser and E.W. Kolb, *Cosmology of Biased Discrete Symmetry Breaking*, *Phys. Rev. D* **39** (1989) 1558 [[INSPIRE](#)].
- [84] S.M. Barr and D. Seckel, *Planck scale corrections to axion models*, *Phys. Rev. D* **46** (1992) 539 [[INSPIRE](#)].
- [85] M. Kamionkowski and J. March-Russell, *Planck scale physics and the Peccei-Quinn mechanism*, *Phys. Lett. B* **282** (1992) 137 [[hep-th/9202003](#)] [[INSPIRE](#)].
- [86] G.B. Gelmini, S. Pascoli, E. Vitagliano and Y.-L. Zhou, *Gravitational wave signatures from discrete flavor symmetries*, *JCAP* **02** (2021) 032 [[arXiv:2009.01903](#)] [[INSPIRE](#)].
- [87] G.B. Gelmini, A. Simpson and E. Vitagliano, *Gravitational waves from axionlike particle cosmic string-wall networks*, *Phys. Rev. D* **104** (2021) 061301 [[arXiv:2103.07625](#)] [[INSPIRE](#)].
- [88] M.P. Hertzberg, M. Tegmark and F. Wilczek, *Axion Cosmology and the Energy Scale of Inflation*, *Phys. Rev. D* **78** (2008) 083507 [[arXiv:0807.1726](#)] [[INSPIRE](#)].
- [89] PLANCK collaboration, *Planck 2018 results. VI. Cosmological parameters*, *Astron. Astrophys.* **641** (2020) A6 [*Erratum ibid.* **652** (2021) C4] [[arXiv:1807.06209](#)] [[INSPIRE](#)].
- [90] K. Saikawa and S. Shirai, *Primordial gravitational waves, precisely: The role of thermodynamics in the Standard Model*, *JCAP* **05** (2018) 035 [[arXiv:1803.01038](#)] [[INSPIRE](#)].
- [91] M.C. Huang and P. Sikivie, *The Structure of Axionic Domain Walls*, *Phys. Rev. D* **32** (1985) 1560 [[INSPIRE](#)].
- [92] S. Blasi et al., *Friction on ALP domain walls and gravitational waves*, *JCAP* **04** (2023) 008 [[arXiv:2210.14246](#)] [[INSPIRE](#)].

- [93] R. Zambujal Ferreira, A. Notari, O. Pujolàs and F. Rompineve, *High Quality QCD Axion at Gravitational Wave Observatories*, *Phys. Rev. Lett.* **128** (2022) 141101 [[arXiv:2107.07542](#)] [[INSPIRE](#)].
- [94] S. Chang, C. Hagmann and P. Sikivie, *Studies of the motion and decay of axion walls bounded by strings*, *Phys. Rev. D* **59** (1999) 023505 [[hep-ph/9807374](#)] [[INSPIRE](#)].
- [95] T. Hiramatsu, M. Kawasaki and K. Saikawa, *Gravitational Waves from Collapsing Domain Walls*, *JCAP* **05** (2010) 032 [[arXiv:1002.1555](#)] [[INSPIRE](#)].
- [96] T. Hiramatsu, M. Kawasaki and K. Saikawa, *On the estimation of gravitational wave spectrum from cosmic domain walls*, *JCAP* **02** (2014) 031 [[arXiv:1309.5001](#)] [[INSPIRE](#)].
- [97] M. Kawasaki and K. Saikawa, *Study of gravitational radiation from cosmic domain walls*, *JCAP* **09** (2011) 008 [[arXiv:1102.5628](#)] [[INSPIRE](#)].
- [98] T. Hiramatsu, M. Kawasaki, K. Saikawa and T. Sekiguchi, *Axion cosmology with long-lived domain walls*, *JCAP* **01** (2013) 001 [[arXiv:1207.3166](#)] [[INSPIRE](#)].
- [99] M. Maggiore, *Gravitational Waves. Vol. 1: Theory and Experiments*, Oxford University Press (2007) [[DOI:10.1093/acprof:oso/9780198570745.001.0001](#)] [[INSPIRE](#)].
- [100] C.-F. Chang and Y. Cui, *Stochastic Gravitational Wave Background from Global Cosmic Strings*, *Phys. Dark Univ.* **29** (2020) 100604 [[arXiv:1910.04781](#)] [[INSPIRE](#)].
- [101] Y. Gouttenoire, G. Servant and P. Simakachorn, *Beyond the Standard Models with Cosmic Strings*, *JCAP* **07** (2020) 032 [[arXiv:1912.02569](#)] [[INSPIRE](#)].
- [102] M. Gorghetto, E. Hardy and H. Nicolaescu, *Observing invisible axions with gravitational waves*, *JCAP* **06** (2021) 034 [[arXiv:2101.11007](#)] [[INSPIRE](#)].
- [103] B. Sathyaprakash et al., *Scientific Objectives of Einstein Telescope*, *Class. Quant. Grav.* **29** (2012) 124013 [*Erratum ibid.* **30** (2013) 079501] [[arXiv:1206.0331](#)] [[INSPIRE](#)].
- [104] F. Ferrer et al., *Primordial Black Holes from the QCD axion*, *Phys. Rev. Lett.* **122** (2019) 101301 [[arXiv:1807.01707](#)] [[INSPIRE](#)].
- [105] M. Kawasaki, K. Saikawa and T. Sekiguchi, *Axion dark matter from topological defects*, *Phys. Rev. D* **91** (2015) 065014 [[arXiv:1412.0789](#)] [[INSPIRE](#)].
- [106] L.M. Widrow, *The Collapse of Nearly Spherical Domain Walls*, *Phys. Rev. D* **39** (1989) 3576 [[INSPIRE](#)].
- [107] R. Laha, *Primordial Black Holes as a Dark Matter Candidate Are Severely Constrained by the Galactic Center 511 keV γ -Ray Line*, *Phys. Rev. Lett.* **123** (2019) 251101 [[arXiv:1906.09994](#)] [[INSPIRE](#)].
- [108] R. Laha, J.B. Muñoz and T.R. Slatyer, *INTEGRAL constraints on primordial black holes and particle dark matter*, *Phys. Rev. D* **101** (2020) 123514 [[arXiv:2004.00627](#)] [[INSPIRE](#)].
- [109] S. Clark et al., *Planck Constraint on Relic Primordial Black Holes*, *Phys. Rev. D* **95** (2017) 083006 [[arXiv:1612.07738](#)] [[INSPIRE](#)].
- [110] S. Mittal, A. Ray, G. Kulkarni and B. Dasgupta, *Constraining primordial black holes as dark matter using the global 21-cm signal with X-ray heating and excess radio background*, *JCAP* **03** (2022) 030 [[arXiv:2107.02190](#)] [[INSPIRE](#)].
- [111] K. Griest, A.M. Cieplak and M.J. Lehner, *Experimental Limits on Primordial Black Hole Dark Matter from the First 2 yr of Kepler Data*, *Astrophys. J.* **786** (2014) 158 [[arXiv:1307.5798](#)] [[INSPIRE](#)].
- [112] MACHO collaboration, *MACHO project limits on black hole dark matter in the 1–30 solar mass range*, *Astrophys. J. Lett.* **550** (2001) L169 [[astro-ph/0011506](#)] [[INSPIRE](#)].

- [113] P.D. Serpico, V. Poulin, D. Inman and K. Kohri, *Cosmic microwave background bounds on primordial black holes including dark matter halo accretion*, *Phys. Rev. Res.* **2** (2020) 023204 [[arXiv:2002.10771](#)] [[INSPIRE](#)].
- [114] P. Lu et al., *Constraining Primordial Black Holes with Dwarf Galaxy Heating*, *Astrophys. J. Lett.* **908** (2021) L23 [[arXiv:2007.02213](#)] [[INSPIRE](#)].
- [115] V. Takhistov et al., *Impacts of Jets and winds from primordial black holes*, *Mon. Not. Roy. Astron. Soc.* **517** (2022) L1 [[arXiv:2111.08699](#)] [[INSPIRE](#)].
- [116] A.K. Saha and R. Laha, *Sensitivities on nonspinning and spinning primordial black hole dark matter with global 21-cm troughs*, *Phys. Rev. D* **105** (2022) 103026 [[arXiv:2112.10794](#)] [[INSPIRE](#)].
- [117] A. Ray, R. Laha, J.B. Muñoz and R. Caputo, *Near future MeV telescopes can discover asteroid-mass primordial black hole dark matter*, *Phys. Rev. D* **104** (2021) 023516 [[arXiv:2102.06714](#)] [[INSPIRE](#)].
- [118] M. Sasaki, T. Suyama, T. Tanaka and S. Yokoyama, *Primordial Black Hole Scenario for the Gravitational-Wave Event GW150914*, *Phys. Rev. Lett.* **117** (2016) 061101 [Erratum *ibid.* **121** (2018) 059901] [[arXiv:1603.08338](#)] [[INSPIRE](#)].
- [119] TIANQIN collaboration, *TianQin: a space-borne gravitational wave detector*, *Class. Quant. Grav.* **33** (2016) 035010 [[arXiv:1512.02076](#)] [[INSPIRE](#)].
- [120] W.-H. Ruan, Z.-K. Guo, R.-G. Cai and Y.-Z. Zhang, *Taiji program: Gravitational-wave sources*, *Int. J. Mod. Phys. A* **35** (2020) 2050075 [[arXiv:1807.09495](#)] [[INSPIRE](#)].
- [121] LISA collaboration, *Laser Interferometer Space Antenna*, [arXiv:1702.00786](#) [[INSPIRE](#)].
- [122] L. Badurina et al., *AION: An Atom Interferometer Observatory and Network*, *JCAP* **05** (2020) 011 [[arXiv:1911.11755](#)] [[INSPIRE](#)].
- [123] AEDGE collaboration, *AEDGE: Atomic Experiment for Dark Matter and Gravity Exploration in Space*, *EPJ Quant. Technol.* **7** (2020) 6 [[arXiv:1908.00802](#)] [[INSPIRE](#)].
- [124] N. Seto, S. Kawamura and T. Nakamura, *Possibility of direct measurement of the acceleration of the universe using 0.1-Hz band laser interferometer gravitational wave antenna in space*, *Phys. Rev. Lett.* **87** (2001) 221103 [[astro-ph/0108011](#)] [[INSPIRE](#)].
- [125] V. Corbin and N.J. Cornish, *Detecting the cosmic gravitational wave background with the big bang observer*, *Class. Quant. Grav.* **23** (2006) 2435 [[gr-qc/0512039](#)] [[INSPIRE](#)].
- [126] LIGO SCIENTIFIC and VIRGO collaborations, *Search for the isotropic stochastic background using data from Advanced LIGO's second observing run*, *Phys. Rev. D* **100** (2019) 061101 [[arXiv:1903.02886](#)] [[INSPIRE](#)].
- [127] L. Pagano, L. Salvati and A. Melchiorri, *New constraints on primordial gravitational waves from Planck 2015*, *Phys. Lett. B* **760** (2016) 823 [[arXiv:1508.02393](#)] [[INSPIRE](#)].
- [128] C. Caprini, R. Durrer, T. Konstandin and G. Servant, *General Properties of the Gravitational Wave Spectrum from Phase Transitions*, *Phys. Rev. D* **79** (2009) 083519 [[arXiv:0901.1661](#)] [[INSPIRE](#)].
- [129] R.-G. Cai, S. Pi and M. Sasaki, *Universal infrared scaling of gravitational wave background spectra*, *Phys. Rev. D* **102** (2020) 083528 [[arXiv:1909.13728](#)] [[INSPIRE](#)].